Neutron scattering from paramagnetic bcc ^{3}He

H. R. Glyde and S. I. Hernadi
Department of Physics, University of Ottawa, Ottawa, Canada K1N 6N5
(Received 10 August 1981)

The dynamic form factor $S(\vec{Q},\omega)$ of bcc solid ^{3}He in the paramagnetic phase is calculated using the self-consistent-phonon (SCP) theory for comparison with proposed neutron scattering measurements. The magnitude of $S(\vec{Q},\omega)$ is predicted to be 2–3 times smaller than that observed in liquid ^{3}He at saturated vapor pressure but comparable with that expected in liquid ^{3}He near the melting line. Longitudinal phonons should be observable at low scattering wave vectors $Q \lesssim 0.8$ Å^{-1}. Transverse phonons will be more difficult to observe since larger scattering wave vectors outside the first Brillouin zone are usually required to observe transverse phonons. At $Q \gtrsim 2.5$ Å^{-1}, $S(\vec{Q},\omega)$ is dominated by scattering from multiphonons and bcc ^{3}He responds like a gas of weakly interacting particles. Collective spin excitations or critical scattering will be observable only at very small neutron energy transfers (~ 0.1 μeV) and at temperatures near the spin-ordering temperature (~ 1 mK). Comparison with experiment will provide a test of the SCP theory and of the assumption used here to separate the nuclear and spin dynamics.

I. INTRODUCTION

In spite of the large absorption cross section of ^{3}He for neutrons, recent neutron scattering studies at the Institut Laue Langevin[1] and Argonne National Laboratory[2] have demonstrated the existence of collective excitations in liquid ^{3}He. These suggest that the liquid supports the propagation of a zero sound[3,4] mode having a lifetime $\sim 2\times10^{-11}$ sec for wave vectors up to $q \approx 1.2$ Å^{-1}. At $q > 1.2$ Å^{-1} the zero sound mode appears to be rapidly damped and the liquid responds much like a weakly interacting Fermi gas in which single quasiparticle-quasihole excitations dominate. The Argonne neutron studies[2] also observe a peak in the scattering at low energy interpreted as the paramagnon resonance in the ^{3}He nuclear-spin excitations. Several semiphenomenological theories[5–10] now describe these observed excitations in liquid ^{3}He well.

Experiments on ^{3}He under pressure are now proposed both to observe the pressure dependence of the scattering from liquid ^{3}He and to observe the excitations and spin structure in solid ^{3}He. At $p \approx 30$ atm and $T \lesssim 1$ K, ^{3}He solidifies into the bcc phase, which is arguably the most highly anharmonic solid known. The purpose of the present paper is to predict the form of the dynamic form factor, $S(\vec{Q},\omega)$, of solid ^{3}He that will be observed in these experiments. Since bcc ^{3}He is highly anharmonic, a direct comparison of the full $S(\vec{Q},\omega)$ with experiment should be more meaningful than attempting to compare approximate one-phonon properties. Also constructing a pressure sample cell transparent to neutrons is difficult, so we choose bcc ^{3}He at $V = 24$ cm^3/mole formed at the lowest pressures just above the melting line.

Briefly, at $T > 10$ mK, where solid ^{3}He is entirely paramagnetic, the inelastic scattering will be from phonons in a highly anharmonic solid. At T near the nuclear-spin ordering temperature ($T \approx 1$ mK at $V = 24$ cm^3/mole) scattering from spin correlations and critical scattering should be observable in the spin-dependent component of $S(\vec{Q},\omega)$. However, since the nuclear-spin excitations will have energies of the order of the exchange energy, ~ 0.1 μeV, extremely small neutron energy transfers to the solid and high-energy resolution will be required to observe these spin excitations. The exchange constant is largest in the bcc phase near melting. Below the ordering temperature the nuclear spins order into complicated antiferromagnetic structures[11–14] which depend upon the applied field.[15] The precise nature of the spin-ordered structures can be determined by an elastic scattering measurement,[16] and identifying the spin structure below $T = 1$ mK is one of the ultimate goals in studying bcc ^{3}He. There are, however, formidable technical difficulties to maintaining these low temperatures in a strong neutron absorber like ^{3}He, so we limit ourselves here to a prediction of scattering from the paramagnetic phase at higher temperature as a first step.

All descriptions of the nuclear dynamics in solid helium use the self-consistent phonon theory,[17] the phonons constituting the long-range dynamic correlations. This is a first-principle theory which has as input only the bare He-He pair interaction potential (represented here by the Beck[18] potential) and the observed lattice parameter (here $a_0 = 4.3034$ Å). The different descriptions of solid helium[19] differ in the treatment of the short-range dynamic correlations in-

duced by the hard core of the He-He potential. In the present calculations we use the T-matrix treatment of these correlations developed by Glyde and Khanna.[20] In the self-consistent phonon theory, solid ^{3}He and ^{4}He are treated on the same footing. This means spin and statistics are ignored in solid ^{3}He when discussing the nuclear dynamics. This approximation is based on the small size of the exchange constant ($\lesssim 1$ mK) compared to the ground-state energy (~ 1 K) and the phonon energies (~ 10–30 K).

Since the nuclear dynamics of solid ^{3}He and ^{4}He are expected to be similar, the extensive neutron studies of solid ^{4}He in the hcp,[21,22] fcc,[23–25] and bcc[26] structures carried out at the Brookhaven[21,24,26] and Ames[22,23,25] laboratories can be used to infer the essential features in solid ^{3}He. The chief new feature in solid ^{3}He is the spin dependence of the ^{3}He neutron scattering length which adds a spin-dependent scattering component to $S(\vec{Q},\omega)$. This makes up $\sim 20\%$ of the scattering in ^{3}He and has no analogy in ^{4}He. The coherent component of $S(\vec{Q},\omega)$ in bcc ^{3}He ($\sim 80\%$ of the scattering) should be very similar to $S(\vec{Q},\omega)$ in bcc ^{4}He, although ^{3}He should be more anharmonic. The essential features of bcc ^{4}He are[26] (1) highly anharmonic one-phonon scattering at small momentum transfer $Q < 1.5$ Å^{-1}, (2) strong interference effects[27–33] between the one-phonon and multiphonon scattering at intermediate momentum transfer 1.5 Å$^{-1} < Q < 3.0$ Å^{-1}, and scattering dominated by multiphonon excitation at large momentum transfer $Q > 3$ Å^{-1}. The scattering from multiphonon excitations at large Q is indistinguishable in form from scattering from nearly free nuclei. Thus, at $Q > 3$ Å^{-1}, solid ^{4}He responds like a gas of weakly interacting "single-particle" ^{4}He atoms[34] and the scattering can be well described by liquidlike theories.[35]

In Sec. II the scattering cross section for solid ^{3}He is separated into its coherent and spin-dependent parts. The calculation of the coherent and spin-dependent $S(\vec{Q},\omega)$ is discussed in Sec. III and the results are presented and discussed in Secs. IV and V, respectively.

II. SCATTERING CROSS SECTION

A. Coherent and spin-dependent parts

The basic expression for the cross section for scattering of neutrons from condensed ^{3}He is the same in the liquid and solid phases. Following the development for liquid ^{3}He, the differential scattering cross section per unit outgoing solid angle Ω and outgoing energy E is[1,2,36,37]

$$\frac{d^2\sigma}{d\Omega\, dE} = \frac{N}{\hbar}\left(\frac{\sigma}{4\pi}\right)\frac{|k|}{|k_0|}S(\vec{Q},\omega) \quad , \tag{1}$$

where

$$S(\vec{Q},\omega) = \frac{\sigma_c}{\sigma}S_c(\vec{Q},\omega) + \frac{\sigma_i}{\sigma}S_I(\vec{Q},\omega) \quad . \tag{2}$$

For an unpolarized incoming neutron beam, the dynamic form factor $S(\vec{Q},\omega)$ separates into a coherent, $S_c(\vec{Q},\omega)$, and a spin-dependent, $S_I(\vec{Q},\omega)$, part. In (1) $\hbar\vec{Q} = \hbar(\vec{k}_0 - \vec{k})$ and $\hbar\omega$ are the momentum and energy transferred from the neutron to the sample, respectively, and the neutron -^{3}He nucleus interaction is represented by a Fermi s-wave pseudopotential, which is spin dependent. (All other interactions are ignored.) Here we use coherent and incoherent bound nucleus scattering cross sections of $\sigma_c = 4.9$ b (Ref. 38) and $\sigma_i = 1.2$ b, giving $\sigma = \sigma_c + \sigma_i = 6.1$ b. The σ_i is not well determined but a careful analysis by Sköld and Pelizzari[2] suggests $\sigma_i/\sigma_c = 0.25 \pm 0.05$.

In (2) $S_c(\vec{Q},\omega)$ is the standard coherent dynamic form factor[39]

$$S_c(\vec{Q},\omega) = \frac{1}{2\pi}\int dt\, e^{i\omega t}\frac{1}{N}\langle \rho(\vec{Q},t)\rho(-\vec{Q},0)\rangle \quad , \tag{3}$$

where

$$\rho(\vec{Q},t) = \sum_l \exp[-i\vec{Q}\cdot\vec{r}(l,t)] \tag{4}$$

is the Qth Fourier component of the nuclear density and $\vec{r}(l)$ is the position of nucleus l. The $S_c(\vec{Q},\omega)$ satisfies the f-sum rule

$$\int_{-\infty}^{\infty} d\omega\, \omega S_c(\vec{Q},\omega) = \frac{\hbar Q^2}{2m} = \omega_R \quad , \tag{5}$$

where ω_R is the recoil frequency in the impulse approximation.

The $S_I(\vec{Q},\omega)$ is the dynamic form factor describing the scattering from the nuclear-spin density

$$S_I(\vec{Q},\omega) = \frac{1}{2\pi}\int dt\, e^{i\omega t}\frac{1}{NI(I+1)} \times \sum_\alpha \langle I_\alpha(\vec{Q},t) I_\alpha(-\vec{Q},0)\rangle \quad , \tag{6}$$

where

$$I_\alpha(\vec{Q},t) = \sum_l I_\alpha(l,t)\exp[-i\vec{Q}\cdot\vec{r}(l,t)] \tag{7}$$

is the Qth Fourier component of this density in the α direction and $\vec{I}(l)$ is the spin of nucleus l. The $S_I(\vec{Q},\omega)$ is the same as the sum of the diagonal components of the dynamic form factor describing the scattering of neutrons from the spin magnetic moments of electrons.[40] If there are correlations among the spins, $S_I(\vec{Q},\omega)$ does not necessarily satisfy the f-sum rule. From the point of view of solids, ^{3}He has two new features. Firstly, the ^{3}He nucleus has a large absorption cross section for neutrons ($\sigma_a \approx 11000$ b at $\lambda_n \approx 4$ Å). Hence absorption will

be most important and will limit the temperatures obtainable and the accuracy obtainable in any scattering measurement. In the case of liquid ^{3}He the corrections necessary for absorption[1,2,36] were carefully applied and experimental results for scattering only were presented. We will assume similar absorption corrections will be applied for solid ^{3}He and have considered only scattering in (1). Secondly, there is the spin-dependent component $S_I(\vec{Q},\omega)$ not present in spinless systems such as ^{4}He.

B. Spin-dependent scattering

When $S_I(\vec{Q},\omega)$ in (6) describes the magnetic scattering of neutrons from electrons it is usual to assume that the electron spin and atomic position expectation values can be evaluated independently.[40] This is because the electron-spin states are largely independent of the position of the nuclei. When $I_\alpha(t)$ refers to nuclear spins in solid ^{3}He it is not so clear that the nuclear-spin values are independent of the nuclear positions. This is particularly true since the origin of the exchange interaction between neighbors in solid ^{3}He arises from the overlap of the nuclear vibrational wave function of one nucleus onto that of its neighbors. Hence, in principle and at some level of detail, the dynamics of the spins and the nuclei are interdependent. However, in all treatments of the dynamics of nuclear motions (phonons) in solid ^{3}He to date,[19] any coupling with the spin dynamics has been ignored. Similarly, most treatments of spin dynamics and evaluations of exchange[41] ignore the phonon dynamics. An example of an exception is the work of Nosanow and Varma[42] who introduced an exchange operator and evaluated the operator in the crystal phonon states to predict exchange constants and spin transitions.

To separate the spin and nuclear dynamics in $S_I(\vec{Q},\omega)$ we recognize that there are two quite separate time and energy scales involved. The phonon frequencies are $\sim 10^{12}$ sec^{-1} while the spin exchange constant is $\sim 10^7$ sec^{-1}. This means that the spin dynamics and spin-flip processes take place $\sim 10^5$ times slower than the nuclear dynamics. Hence to study spin motion, the time scale needed is so long from the point of view of nuclear motion that we can approximate t by $t=\infty$ in the nuclear positions $\vec{r}(l,t)$ in $S_I(\vec{Q},\omega)$. This means we need keep only the elastic component of the nuclear scattering when discussing the spin dynamics.

The same argument may be made more precise using an energy scale basis. The phonon energies are ~ 10–30 K~ 1–3 meV while the exchange energy is ~ 1 mK~ 0.1 μeV. We can then consider two quite separate energy transfer regions ($\hbar\omega$) in $S_I(\vec{Q},\omega)$. If we study phonons we must transfer enough energy from the neutron to the crystal to create a phonon, i.e., 1–3 meV. On this energy scale any changes in the spin system or contributions from the spin dynamics will be unobservably small. For practical purposes we can evaluate the nuclear dynamics independently. Similarly, at low enough energy transfers ($\lesssim 1$ μeV) to study the spin dynamics there is not enough energy transferred to create (or absorb) a phonon. The energy transfer is sufficiently small that we are in the elastic region ($\hbar\omega=0$) so far as the nuclear dynamics is concerned.

To formalize this separation of the spin and nuclear dynamics on the basis of differing energy transfer scales, we extract the elastic nuclear component

$$S_I(\vec{Q},\omega)_{\rm el}=\frac{1}{2\pi}\int_{-\infty}^{\infty}dt\,e^{i\omega t}\frac{1}{I(I+1)}\sum_{l}\exp[i\vec{q}\cdot\vec{R}(l0)]d^2(Q)\sum_{\alpha}\langle I_\alpha(l,t)I_\alpha(0,0)\rangle \tag{8}$$

from (6), where $d(Q)$ is the Debye-Waller factor and $R(l0)=R(l)-R(0)$ are lattice point positions. The remaining inelastic part will require neutron energy transfers $\hbar\omega\sim 10^4-10^5$, the exchange energy to excite, and on this energy scale any contributions from coupling with the spin system will be unobservable. Hence, when energy transfers large enough to excite and study phonons are used, the nuclear expectation values can be evaluated independently of the spin states for all practical purposes and

$$S_I(\vec{Q},\omega)\approx\frac{1}{2\pi}\int dt\,e^{i\omega t}\frac{1}{NI(I+1)}\sum_{ll'}\langle\exp[-i\vec{Q}\cdot\vec{r}(l,t)]\exp[i\vec{Q}\cdot\vec{r}(l',0)]\rangle\sum_{\alpha}\langle I_\alpha(l,t)I_\alpha(l',0)\rangle\ . \tag{9}$$

This argument is not quite exact for multiphonon excitations which can have contributions at $\omega\approx 0$, but again for practical purposes this will be unimportant. This separation should be valid for all spin phases of solid ^{3}He and when we wish to study spin dynamics, where the energy transfer will be $\sim 10^{-4}$–10^{-5} the one-phonon energy, we can approximate the space expectation value by its elastic part and use (8).

For paramagnetic ^{3}He ($T\gtrsim 2$ mK)

$$\langle I_\alpha(l,t)I_\alpha(l',0)\rangle=\tfrac{1}{3}I(I+1)\delta_{ll'}\ . \tag{10}$$

That is, the expectation value is independent of time and direction. In this simple case $S_I(\vec{Q},\omega)$ reduces

to the usual incoherent result for phonons

$$S_I(\vec{Q},\omega)=\frac{1}{2\pi}\int dt\, e^{i\omega t}\langle\exp[-i\vec{Q}\cdot\vec{r}(t)]\exp[i\vec{Q}\cdot\vec{r}(0)]\rangle \ . \tag{11}$$

This $S_I(\vec{Q},\omega)$ will be valid for all energy transfers except for $\hbar\omega\lesssim 1$ μeV at T near 2 mK, where spin correlations will become important and observable. The $S_I(\vec{Q},\omega)$ in (11) now satisfies the f-sum rule.

III. DYNAMIC FORM FACTORS

A. Coherent part

To evaluate $S_c(\vec{Q},\omega)$ we expand it in terms of scattering from single phonons, pairs of phonons and so on in the usual way,[27,28]

$$S_c(\vec{Q},\omega)=S_0(\vec{Q})+S_p(\vec{Q},\omega)+S_2(\vec{Q},\omega)+S_3(\vec{Q},\omega)+\ldots \ . \tag{12}$$

Here $S_0(\vec{Q})=Nd^2(Q)\Delta(\vec{Q})\delta(\omega)$ is the elastic scattering component and $S_p(\vec{Q},\omega)$ describes the scattering in which one phonon is created or destroyed. This includes possible interference processes between one-phonon and multiphonon scattering. In the present calculation we include only the interference between the one- and two-phonon scattering processes so that

$$S_p(\vec{Q},\omega)=S_1(\vec{Q},\omega)+S_{12}(\vec{Q},\omega) \ , \tag{13}$$

where

$$S_1(\vec{Q},\omega)=\frac{1}{2\pi}\Delta(\vec{Q}-\vec{q})\sum_{\lambda}[F(\vec{Q},\vec{q}\lambda)]^2\times[n(\omega)+1]A(q\lambda,\omega) \tag{14}$$

is the pure one-phonon part and $S_{12}(\vec{Q},\omega)$ is the interference term documented elsewhere.[27–29,32,33] In $S_1(\vec{Q},\omega)$,

$$F(\vec{Q},\vec{q}\lambda)=d(Q)\left[\frac{\hbar}{2m\omega_{q\lambda}}\right]^{1/2}(\vec{Q}\cdot\vec{\epsilon}_{q\lambda}) \tag{15}$$

is the structure factor, where $\omega_{q\lambda}$ and $\epsilon_{q\lambda}$ are the frequency and polarization of phonon having wave vector $\vec{q}$ and branch λ created in the scattering, $n(\omega)$ is the Bose function and m is the ^{3}He atomic mass. The $A(q\lambda,\omega)$ is the one-phonon response function,

$$A(q\lambda,\omega)=8\omega_{q\lambda}^2\Gamma(q\lambda,\omega)/\{[-\omega^2+\omega_{q\lambda}^2+2\omega_{q\lambda}\Delta(q\lambda,\omega)]^2+[2\omega_{q\lambda}\Gamma(q\lambda,\omega)]^2\} \ , \tag{16}$$

and Δ and Γ are the phonon frequency shift and inverse lifetime due to anharmonic terms. The $A(q\lambda,\omega)$ is approximately a Lorentzian function and the position of its peak is usually taken as the one-phonon frequency.

For harmoniclike phonons having infinite lifetime the two-phonon scattering component is

$$S_2(\vec{Q},\omega)=\frac{1}{2\pi N}\sum_{1,2}[F(\vec{Q},1)]^2[F(\vec{Q},2)]^2[n(\omega)+1]J(1,2,\omega)\Delta(\vec{Q}-\vec{q}_1-\vec{q}_2) \ , \tag{17}$$

where $J(1,2,\omega)$ is the two-phonon density of states and $1=q_1\lambda_1$.

The expansion (12) implies a phonon model and to evaluate $S_c(\vec{Q},\omega)$ we need a single phonon frequency $\omega_{q\lambda}$ which best represents the anharmonic phonons in solid ^{3}He. To obtain this frequency we first calculate $S_1(\vec{Q},\omega)$ using the self-consistent harmonic (SCH) frequencies of Glyde and Khanna[20] with Δ and Γ in (16) given by the cubic anharmonic term. The resulting S_1 (and S_p and S_2) is shown in Fig. 1. From $S_1(\vec{Q},\omega)$ we define, following Horner,[43] a mean one-phonon frequency,

$$\hat{\omega}_{q\lambda}=\int_{-\infty}^{\infty}d\omega\,\omega S_1(\vec{Q},\omega)\Big/\int_{-\infty}^{\infty}d\omega\,S_1(\vec{Q},\omega) \ , \tag{18}$$

for each phonon $q\lambda$. This $\hat{\omega}_{q\lambda}$ represents the frequency of a harmoniclike approximation to the anharmonic $S_1(\vec{Q},\omega)$. This definition is identical to imposing a harmoniclike form on $A(q\lambda,\omega)$,

$$A(q\lambda,\omega)=2\pi[\delta(\omega-\hat{\omega}_{q\lambda})-\delta(\omega+\hat{\omega}_{q\lambda})] \ ,$$

at $T=0$ K [and at finite T if the integrations in (18) are restricted to run from 0 to ∞]. The $\hat{\omega}_{q\lambda}$ lie somewhat above the positions of the main peak in $S_1(\vec{Q},\omega)$ because the $S_1(\vec{Q},\omega)$ usually has a tail extending up to high frequencies. The $\hat{\omega}_{q\lambda}$ are compared with the peak positions of $S_1(\vec{Q},\omega)$, denoted the SCH+C frequencies, in Fig. 2.

Having obtained the $\hat{\omega}_{q\lambda}$ we use these frequencies as the intermediate propagator frequencies throughout the calculation of $S_c(\vec{Q},\omega)$. We believe these $\hat{\omega}_{q\lambda}$ are the frequencies most representative of

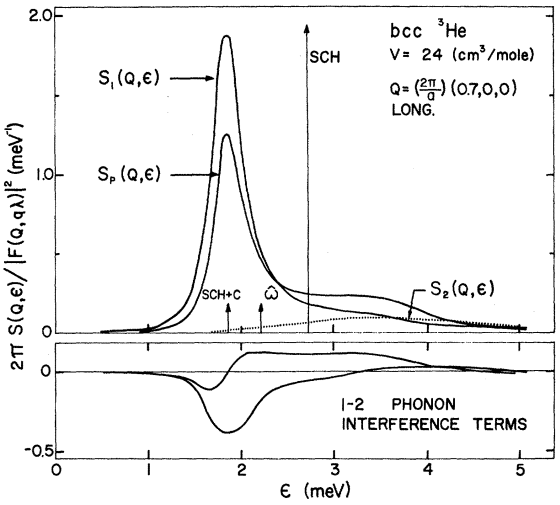

FIG. 1. Components of the coherent dynamic form factor for the longitudinal phonon at $\vec{Q}=(2\pi/a)(0.7,0,0)$: $S_1(\vec{Q},\epsilon)$, the one-phonon part, $S_p(\vec{Q},\epsilon)$, the one-phonon plus interference terms, and $S_2(\vec{Q},\epsilon)$, the two-phonon part, are calculated using the SCH frequencies as intermediate propagator frequencies. The arrows show the position of the corresponding SCH frequency, the SCH+C frequency and the frequency $\hat{\omega}_{q\lambda}$ defined by (18).

solid ^{3}He short of a fully iterative calculation including the phonon linewidths. We do, however, want $S_1(\vec{Q},\omega)$ calculated using the $\hat{\omega}_{q\lambda}$ to peak at approximately the original SCH+C frequency. This means the $\hat{\Delta}(q\lambda,\omega)$ in (16), calculated using the $\hat{\omega}_{q\lambda}$, should be zero when $\omega\approx\hat{\omega}_{q\lambda}$. To achieve this we use

$$\hat{\Delta}_0(q\lambda,\omega)=\hat{\Delta}(q\lambda,\omega)-\hat{\Delta}(q\lambda,\hat{\omega}_{q\lambda})$$

in (16). This $\hat{\Delta}_0(q\lambda,\omega)$ will have zero net value when $\omega=\hat{\omega}_{q\lambda}$, but will have the correct frequency dependence appropriate to the $\hat{\omega}_{q\lambda}$ propagator needed to preserve the Ambegaokar, Conway, and Baym[27] (ACB) and f-sum rules in $S_c(\vec{Q},\omega)$ (see below).

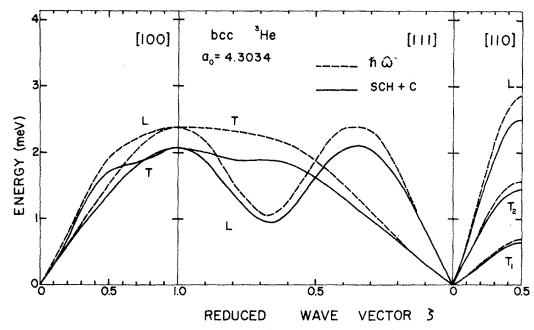

FIG. 2. The SCH+C and $\hbar\hat{\omega}_{q\lambda}$ "phonon" energies for bcc ^{3}He at $V=24$ cm^3/mole.

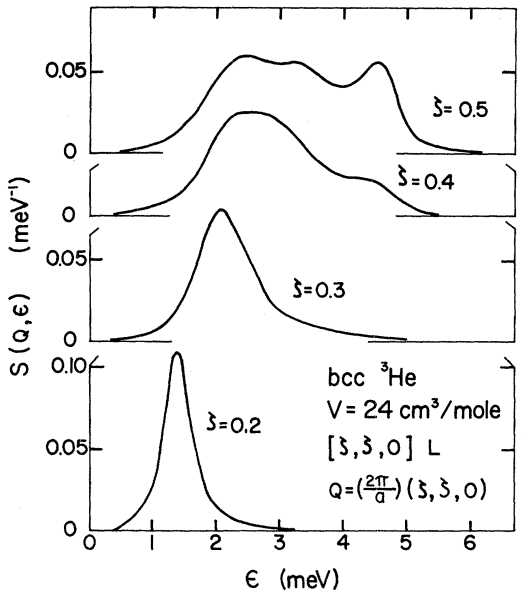

FIG. 3. Coherent $S_p(\vec{Q},\epsilon)+S_2(\vec{Q},\epsilon)$ for longitudinal phonons along the [110] direction.

The S_p+S_2 for longitudinal phonons along the [110] direction calculated using the $\hat{\omega}_{q\lambda}$ frequencies are shown in Fig. 3. From Fig. 3 we see these phonon groups already show extreme anharmonic character even for wave vectors lying within the first Brillouin zone.

The one-phonon component S_p (and S_1) satisfies the ACB sum rule,

$$\int d\omega\,\omega S_p(\vec{Q},\omega)=d^2(Q)\frac{\hbar(\vec{Q}\cdot\vec{\epsilon}_{q\lambda})^2}{2m}\quad.\qquad(19)$$

For scattering vectors adjusted so that $[\vec{Q}\cdot\vec{\epsilon}_{q\lambda}]^2=Q^2$

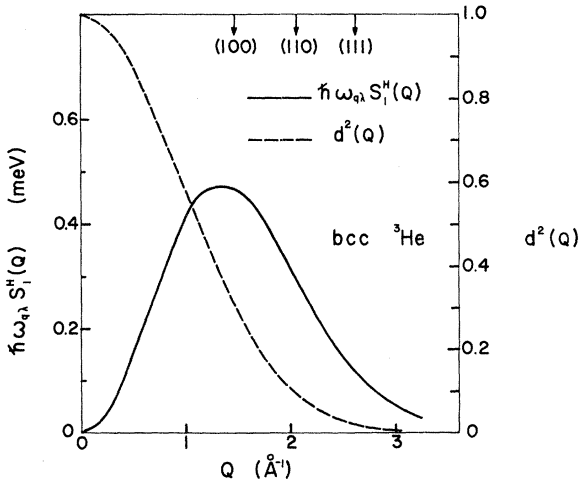

FIG. 4. The square of the Debye-Waller factor, $d^2(Q)$ and the harmonic one-phonon $S_1^H(\vec{Q})$ [proportional to $Q^2d^2(Q)$] predicted for bcc ^{3}He at $V=24$ cm^3/mole.

this shows that the one-phonon component $S_p(\vec{Q},\omega)$ takes up a fraction $d^2(Q)$ of the f-sum rule. In Fig. 4 we have plotted our calculation of $d^2(Q)$ made in Sec. IV. At $Q \approx 2$ Å^{-1}, which is just beyond the edge of the first Brillouin zone, $d^2(Q) \approx 0.1$ and $S_p(\vec{Q},\omega)$ takes up only 10% of the f-sum rule. Clearly $S_p(\vec{Q},\omega)$ makes up only a small part of $S_c(\vec{Q},\omega)$ and higher terms $S_n(\vec{Q},\omega) n > 3$ in (12) will be important. To evaluate these we have made the incoherent approximation

$$\rho(-\vec{Q},0) \approx \rho_s(-\vec{Q},0) = \exp[i\vec{Q}\cdot\vec{r}(l,0)]$$

[in (3)] for $n > 3$ and used the incoherent expression (25) developed in Sec. IV. With the simple expression (25) for $S_n(\vec{Q},\omega)$ we can include enough terms $S_n(\vec{Q},\omega)$, $n > 3$ (say 10–30) to catch all of $S_c(\vec{Q},\omega)$ and exhaust the f-sum rule (5) exactly. The incoherent approximation conserves the f-sum rule.

B. Incoherent part

The traditional way to evaluate $S_I(\vec{Q},\omega)$ in (11) for an anharmonic solid is to expand it in terms of scattering from phonons as for $S_c(\vec{Q},\omega)$. This expansion is simple in the incoherent case since there are no interference terms between the scattering from different numbers of phonons, e.g., between the scattering that creates a single phonon and that which creates many phonons. The interference terms vanish because there is no phonon wave vector selection which requires that the phonon wave vector $\vec{q}$ equals the scattering wave vector $\vec{Q}$ in incoherent scattering [compare Eq. (14)]. A sum over equal numbers of $\pm q$ values remains and since the interference terms are odd functions of q their total contribution to $S_I(\vec{Q},\omega)$ vanishes. On writing $\vec{r} = \vec{R} + \vec{u}$, the expectation value in (11) is

$$\langle \exp[-i\vec{Q}\cdot\vec{u}(t)]\exp[i\vec{Q}\cdot\vec{u}(0)]\rangle = \exp\{-\langle[\vec{Q}\cdot\vec{u}(0)]\rangle^2\}\exp\{\langle[\vec{Q}\cdot\vec{u}(t)][\vec{Q}\cdot\vec{u}(0)]\rangle\} \ , \tag{20}$$

which is the simple harmonic result. This also introduces the harmonic like approximation for the Debye-Waller factor

$$d(Q) = \langle \exp(i\vec{Q}\cdot\vec{u})\rangle \approx \exp(-\tfrac{1}{2}\langle[\vec{Q}\cdot\vec{u}]^2\rangle) \equiv e^{-W} \ . \tag{21}$$

To proceed, we approximate the dynamics by the harmoniclike phonons having frequencies defined in (18). Using the ACB sum rule (19) in the numerator and (14) in the denominator of (18), (18) becomes

$$\hat{\omega}_{q\lambda} \equiv \frac{\omega_{q\lambda}}{\int_{-\infty}^{\infty}\frac{d\omega}{2\pi}[n(\omega)+1]A(q\lambda,\omega)} \ .$$

The general expression for the expectation values appearing in (20) such as

$$2W = \langle[\vec{Q}\cdot\vec{u}(0)]^2\rangle = \frac{1}{N}\sum_{q\lambda}\left(\frac{\hbar}{2m\omega_{q\lambda}}\right)(\vec{Q}\cdot\vec{\epsilon}_{q\lambda})^2 \times \int_{-\infty}^{\infty}\frac{d\omega}{2\pi}[n(\omega)+1]A(q\lambda,\omega) \ ,$$

then reduce to harmonic form

$$2W = \frac{1}{N}\sum_{q\lambda}\left(\frac{\hbar}{2m\hat{\omega}_{q\lambda}}\right)(\vec{Q}\cdot\vec{\epsilon}_{q\lambda})^2 \ .$$

Using the $\hat{\omega}_{q\lambda}$ we can construct a density-of-frequency state $\hat{g}(\omega)$ so that

$$2W = \omega_R\int_0^{\omega_m} d\omega\,\frac{\hat{g}(\omega)}{\omega} \ ,$$

where $\omega_R = \hbar Q^2/2m$ is the recoil frequency and ω_m the maximum frequency $\hat{\omega}_{q\lambda}$ of the crystal. For convenience we also introduce the inverse first moment of $\hat{g}(\omega)$,

$$\omega_I \equiv \int_0^{\omega_m} d\omega\,\frac{\hat{g}(\omega)}{\omega} \ ,$$

and the normalized density function

$$\hat{G}(\omega) = \frac{1}{\omega_I}\frac{\hat{g}(\omega)}{\omega} \ . \tag{22}$$

The function $\hat{G}(\omega)$ is displayed in Fig. 5 and

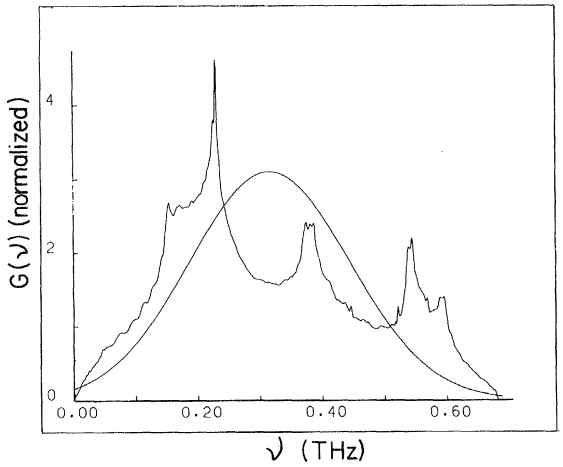

FIG. 5. The normalized density function $G(\nu) = g(\nu)/\nu$ and the Gaussian approximation to it (smooth line) given by (24). For $\nu = 1$ THz, $\epsilon = h\nu = 4.135$ meV.

$\nu_I = 2\pi\omega_I = 3.172$ THz^{-1} giving an equivalent Debye-Waller temperature of $\Theta_{DW} = (3\hbar/2k)/\omega_I = 22.7$ K. In terms of ω_I and $\hat{G}(\omega)$, $2W = \omega_R \omega_I$ and

$$S_I(\vec{Q},\omega) = e^{-2W}\frac{1}{2\pi}\int_{-\infty}^{\infty} dt\, e^{i\omega t}\exp\left[2W\int_0^{\omega_m} d\omega'\,\hat{G}(\omega')e^{-i\omega' t}\right] .$$

We now expand the exponential in $S_I(\vec{Q},\omega)$ to obtain the zero-phonon (elastic), the one-phonon, two-phonon component and so on,

$$S_{I0}(\vec{Q}) = e^{-2W}\delta(\omega) ,$$

$$S_{I1}(\vec{Q},\omega) = e^{-2W}2W\hat{G}(\omega) ,$$

$$S_{I2}(\vec{Q},\omega) = e^{-2W}\tfrac{1}{2}(2W)^2\int_0^{\omega_m} d\omega'\,\hat{G}(\omega')\hat{G}(\omega-\omega') . \tag{23}$$

This series does not converge well at $Q > 2$ Å^{-1} because $2W$ becomes large. To describe the higher orders we approximate $\hat{G}(\omega)$ by a Gaussian function

$$\hat{G}(\omega) = (\alpha/\pi)^{1/2}\exp[-\alpha(\omega-\omega_0)^2] . \tag{24}$$

Here ω_0 fixes the center of $G(\omega)$ and α its width. It is straightforward to show that if $S_I(\vec{Q},\omega)$ is to satisfy the f-sum rule we must choose $\omega_0 = \omega_I^{-1}$. The α is chosen to give a best fit to $\hat{G}(\omega)$ and this fit is shown in Fig. 5. The f-sum rule is independent of α and $S_I(Q)$ is independent of both α and ω_0. The nth term of $S_I(\vec{Q},\omega)$ is then

$$S_{In}(\vec{Q},\omega) = e^{-2W}\frac{1}{n!}(2W)^n\left(\frac{(\alpha/n)}{\pi}\right)^{1/2} \times\exp[-\alpha/n(\omega-n\omega_0)^2] . \tag{25}$$

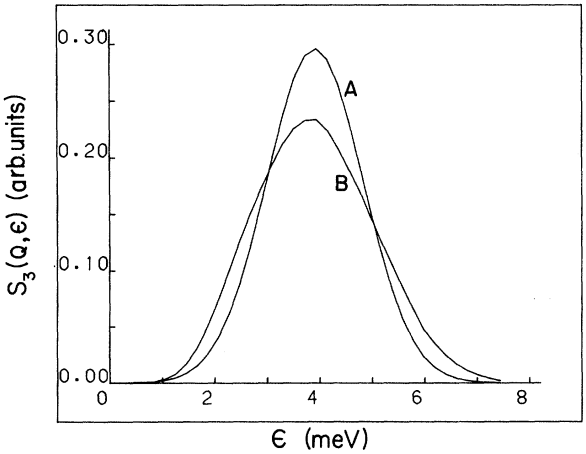

FIG. 6. Three-phonon scattering component $S_3(\vec{Q},\epsilon)$ in the incoherent approximation calculated; A using the density function $G(\nu)$ and B using Gaussian approximation in (24) to $G(\nu)$ both shown in Fig. 5.

To check the validity of this approximation we calculated $S_{I3}(\vec{Q},\omega)$ using the actual $\hat{G}(\omega)$ and the Gaussian approximation to it (24). The two $S_{I3}(\vec{Q},\omega)$ are compared in Fig. 6. The comparison shows there is enough folding over frequencies that both the $S_{I3}(\vec{Q},\omega)$ are of Gaussian form, but that the α we selected is somewhat too large.

To compute $S_I(\vec{Q},\omega)$ we then used

$$S_I(\vec{Q},\omega) = S_{I0}(\vec{Q}) + S_{I1}(\vec{Q},\omega) + S_{I2}(\vec{Q},\omega) + \sum_{n=3}^{\infty} S_{In}(\vec{Q},\omega) , \tag{26}$$

keeping enough terms that the series converged. This $S_I(\vec{Q},\omega)$ exhausts the f-sum rule and

$$\int d\omega\, S_I(\vec{Q},\omega) = S_I(\vec{Q}) = 1 .$$

IV. NUMERICAL RESULTS

A. Longitudinal phonons

Figure 7 shows $S(\vec{Q},\omega)$ for scattering wave vectors $\vec{Q} = 2\pi/a(\zeta,0,0)$ along [100] direction. Two lines are plotted, the full $S(\vec{Q},\epsilon)$ in (2) and the one- and two-phonon parts of the coherent scattering component

$$\sigma_c/\sigma[S_p(\vec{Q},\epsilon) + S_2(\vec{Q},\epsilon)]$$

in (12). Each $S(\vec{Q},\epsilon)$ is folded with a Gaussian function of full width at half maximum (FWHM) $= 0.30$ meV to simulate a finite experimental instrument energy resolution width. At low-Q values we see that $S(\vec{Q},\epsilon)$ is dominated by the one- and two-phonon scattering parts and $S_p(\vec{Q},\epsilon)$ is clearly well described by a Lorentzian function. For $|Q| > 0.8$ Å^{-1}, $S_p(\vec{Q},\epsilon)$ becomes a broader, flatter, and more irregular function and the incoherent and multiphonon scattering contributions to $S(\vec{Q},\epsilon)$ become relatively more important. The wavey form of the total $S(\vec{Q},\epsilon)$ in the energy region $\epsilon = 1-3$ MeV comes from the density-of-phonon states appearing in the incoherent component. The sharp increase at $\epsilon \approx 0$ is the elastic, incoherent scattering. Clearly, well-defined single-phonon energies are observable at small wave vectors near the first Brillouin zone center only.

Figures 8 and 9 show similar plots of $S(\vec{Q},\epsilon)$ for $\vec{Q}$

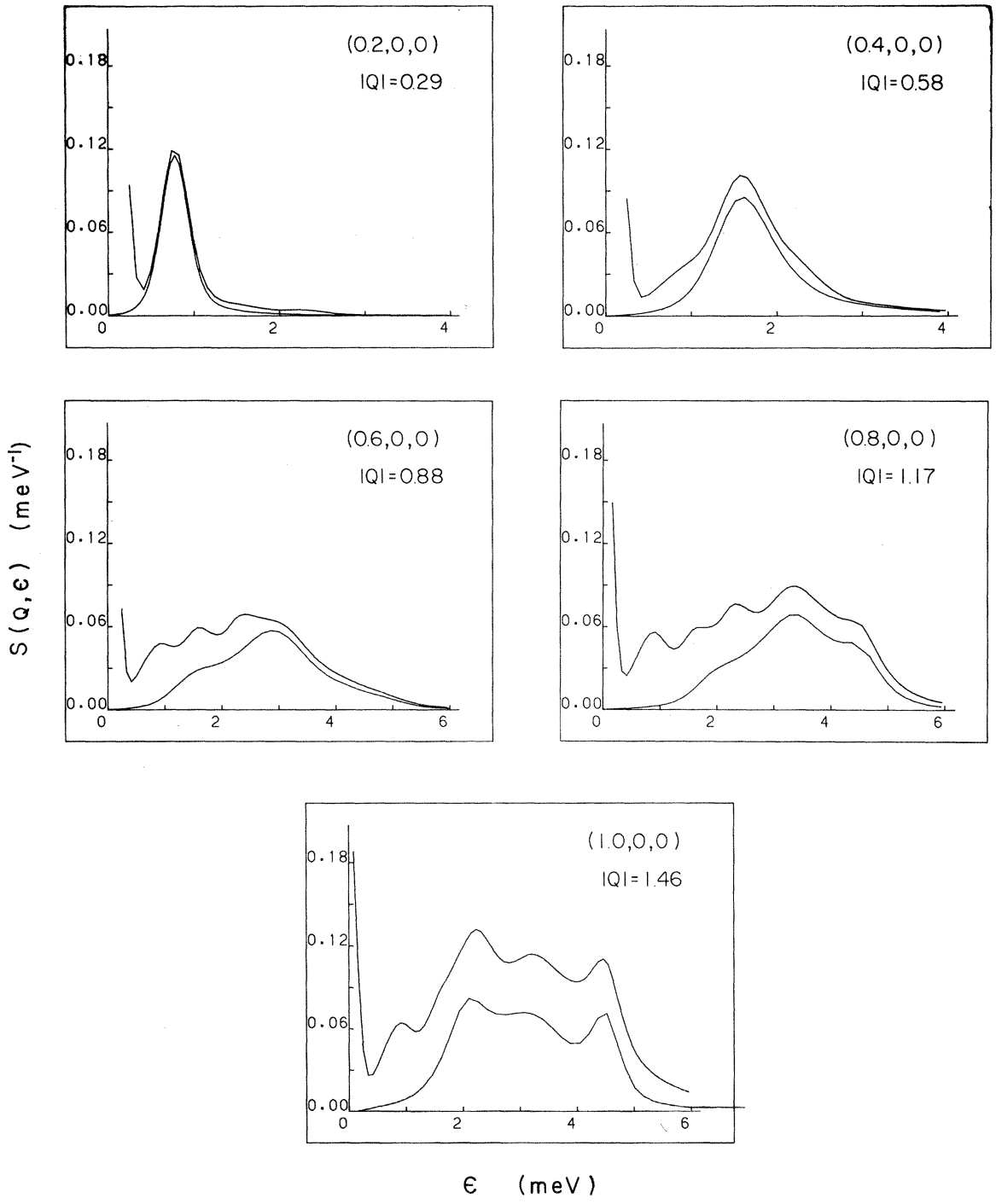

FIG. 7. The $S(\vec{Q}, \epsilon)$ predicted by (2) (upper line) and $\sigma_c/\sigma[S_p(\vec{Q}, \epsilon) + S_2(\vec{Q}, \epsilon)]$ of the coherent part (lower line) for longitudinal phonons along the [100] direction in bcc ^{3}He at $V = 24$ cm^3/mole; $|Q|$ in Å^{-1}.

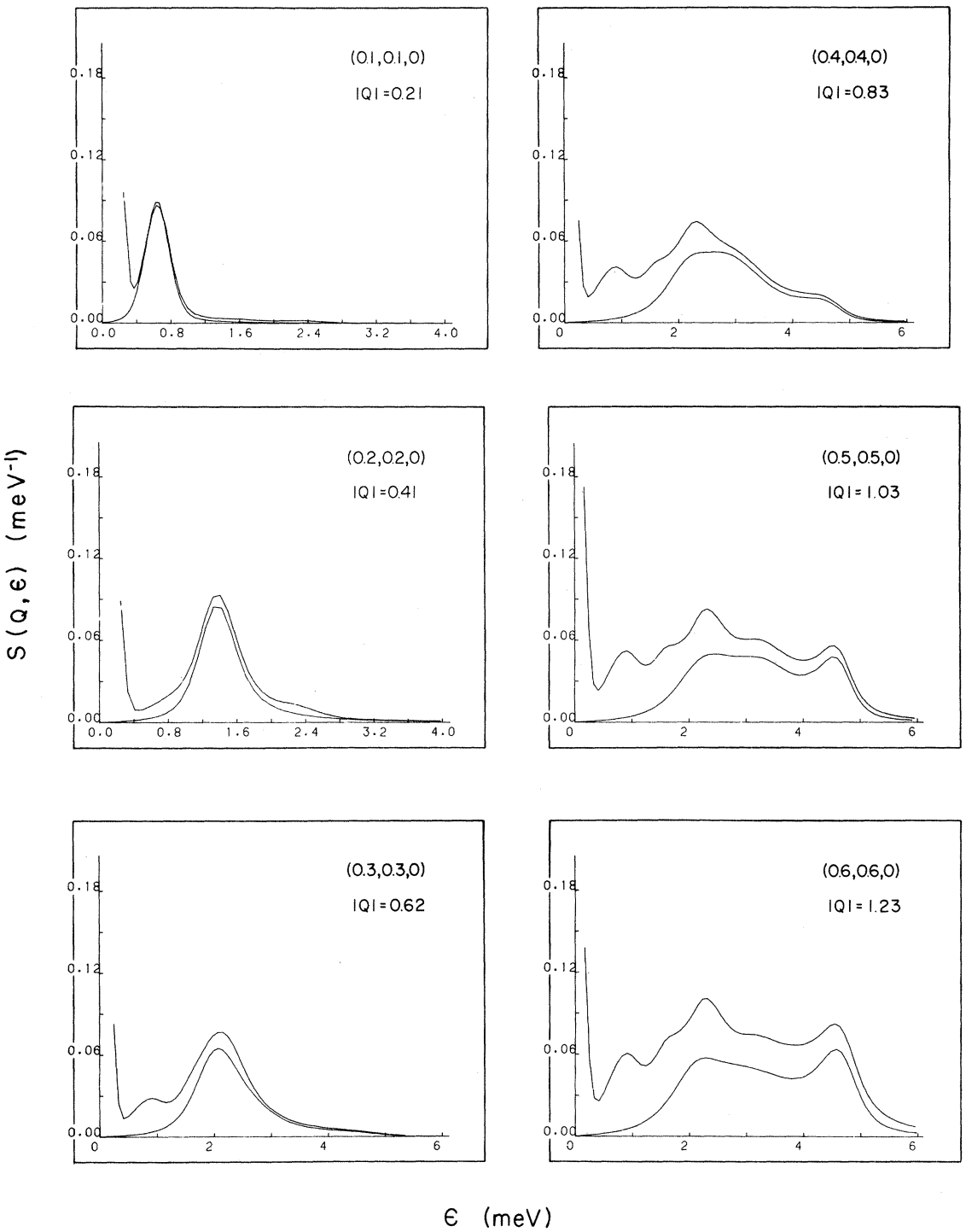

FIG. 8. As Fig. 7 for the [110] direction.

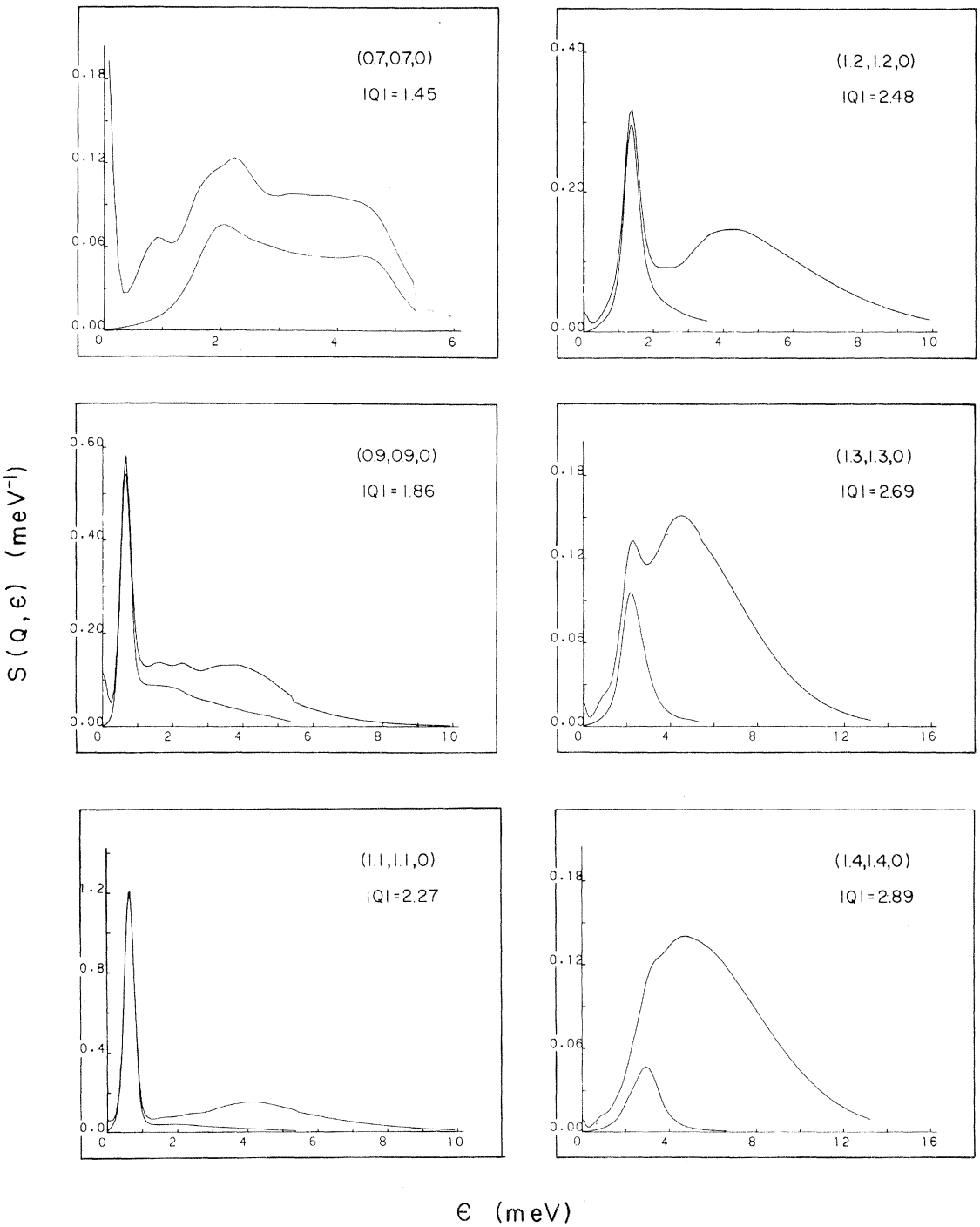
(0.7,0.7,0)
|Q| = 1.45
(1.2,1.2,0)
|Q| = 2.48
(0.9,0.9,0)
|Q| = 1.86
(1.3,1.3,0)
|Q| = 2.69
(1.1,1.1,0)
|Q| = 2.27
(1.4,1.4,0)
|Q| = 2.89
S(Q,ϵ) (meV⁻¹)
ϵ (meV)

FIG. 9. As Fig. 8.

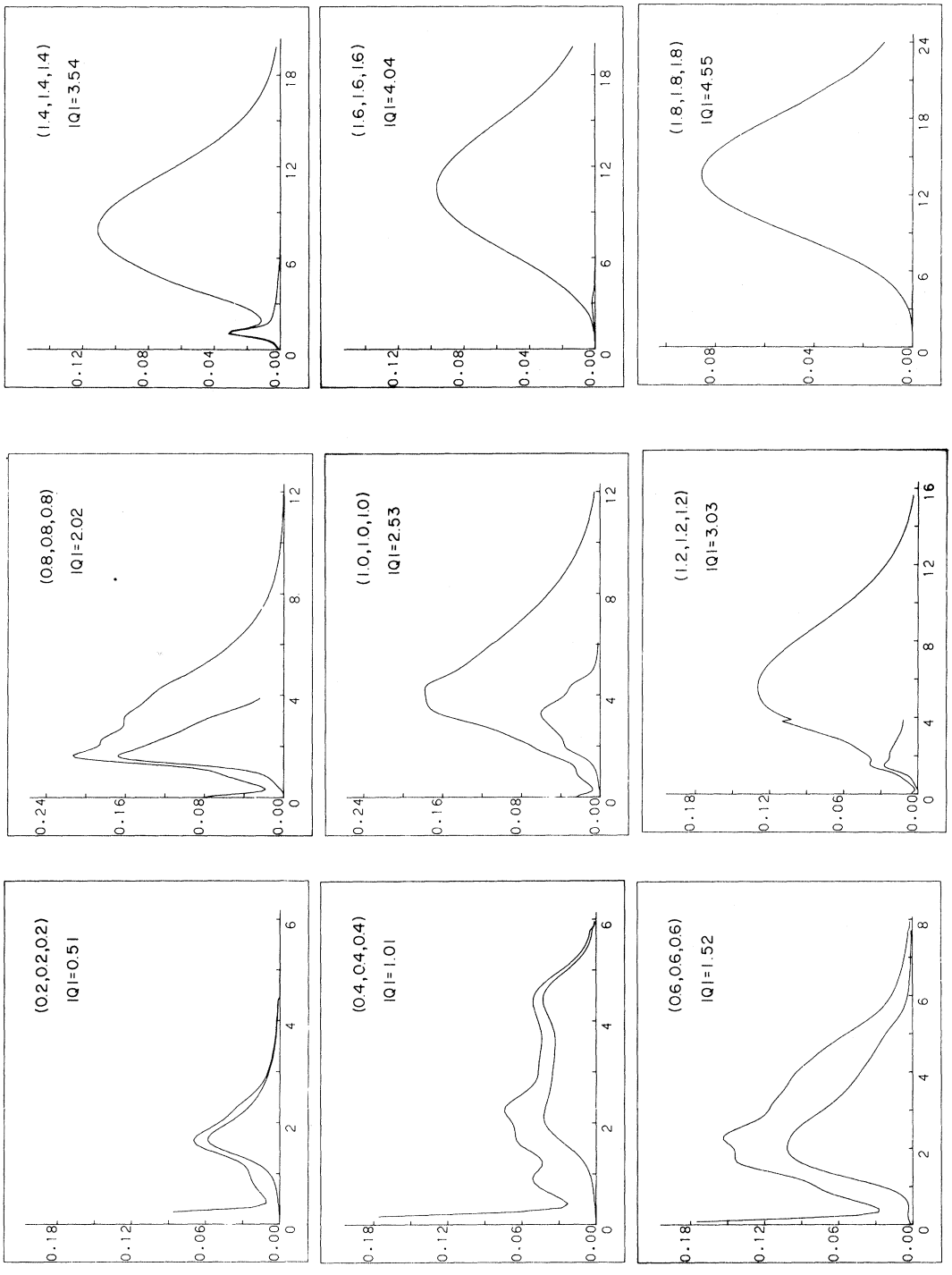

FIG. 10. As Fig. 7 for the [111] direction.

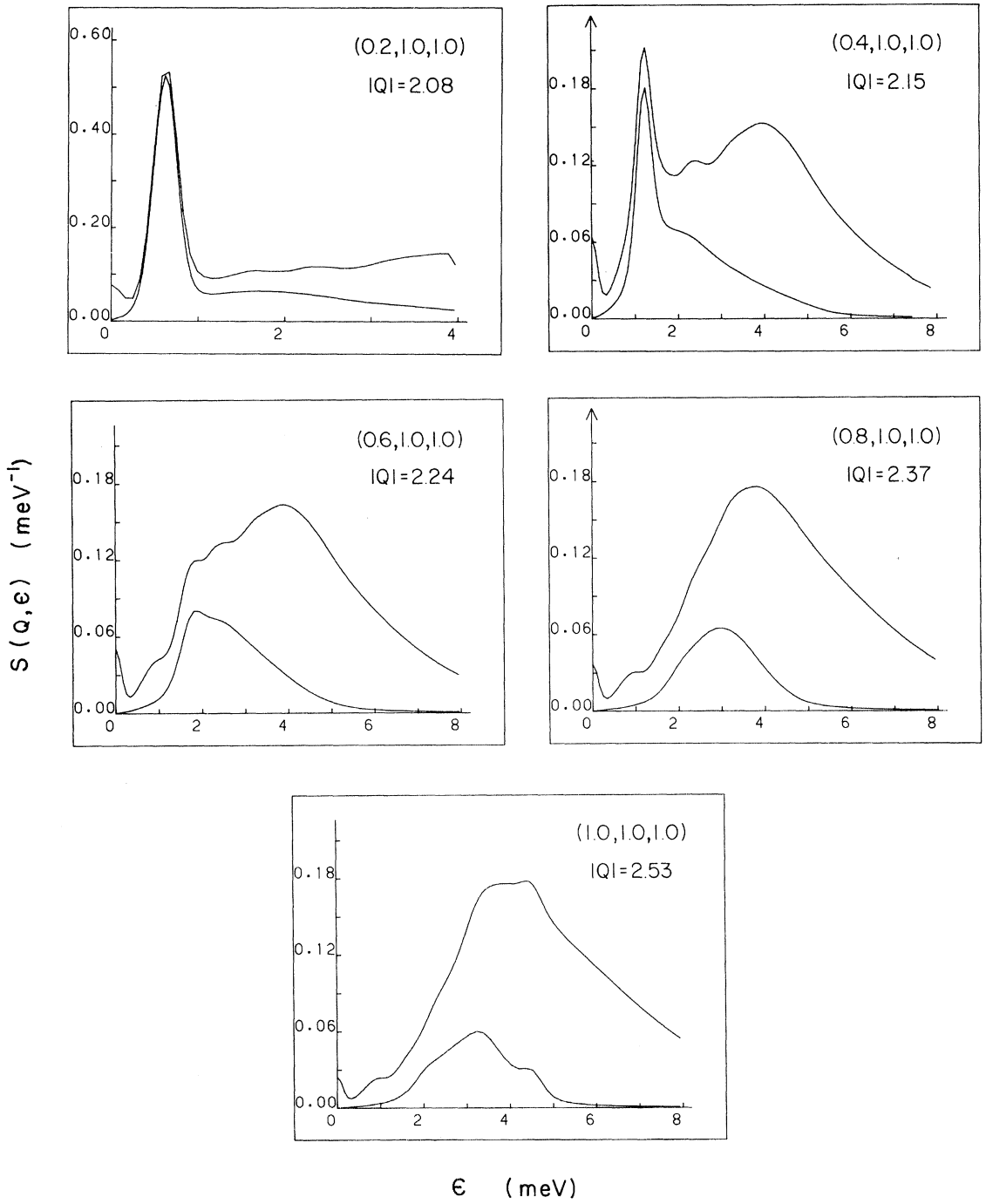

FIG. 11. The $S(\vec{Q}, \epsilon)$ predicted by (2) for transverse phonons observed at $\vec{Q}=(2\pi/a)(\zeta, 1, 1)$, $\zeta=0.2-1.0$.

along the [110] direction. Again we see a well-defined one-phonon scattering contribution for $|Q| \lesssim 0.8$ Å^{-1}, but at higher $|Q|$ the one-phonon scattering becomes diffuse with no well-defined single peak. In the region of the first Bragg point (1,1,0) along this direction, where the one-phonon frequency is small, the one-phonon scattering intensity again dominates and $S(\vec{Q}, \epsilon)$ is collected into a sharply peaked function. At $|Q| \gtrsim 2.5$ Å^{-1}, multiphonon scattering in both the coherent and incoherent parts is beginning to dominate $S(\vec{Q}, \epsilon)$. Figure 10 shows a similar plot of $S(\vec{Q}, \epsilon)$ for $\vec{Q}$ along the [111] direction. This displays clearly that for $|Q| \gtrsim 3.0$ Å^{-1} scattering from multiples of phonons dominates $S(\vec{Q}, \epsilon)$ and the crystal responds much like a gas of weakly interacting, classical ^{3}He atoms.

B. Transverse phonons

Figure 11 displays $S(\vec{Q}, \epsilon)$ for scattering wave vectors $\vec{Q} = (2\pi/a)(\zeta, 1, 1)$ in which the transverse phonon having reduced wave vector $\vec{q} = 2\pi/a\,(\zeta, 0, 0)$ is excited. These calculations suggest that only for $\zeta \leq 0.4$ will a well-defined one-phonon component be observed in this region of scattering wave-vector space. At $\vec{Q} = (2\pi/a)(0.8, 1, 1)$ what looks like a well-defined one-phonon peak is actually a peak in $S_2(\vec{Q}, \omega)$. Figure 12 shows similar plots of $S(\vec{Q}, \epsilon)$ for scattering wave vectors $\vec{Q} = (2\pi/a)(2.\zeta, \zeta, 0)$ in which the transverse phonon along the [110] direction (shown in the dispersion curves in Fig. 2) is excited. Again, only for small values of ζ is a clearly distinguishable one-phonon component apparent. The limited study in Figs. 11 and 12 suggests that scattering from transverse phonons may be difficult to observe because multiphonon scattering dominates at relatively small-Q values. There may, however, be better places in reciprocal space to observe transverse phonons than investigated here.

C. Single-particlelike behavior

As noted, especially in Fig. 10, at $|Q| \gtrsim 2.5$ Å^{-1} solid ^{3}He responds like a gas of weakly interacting "single particles." The calculated $S(\vec{Q}, \epsilon)$ shows a broad Gaussian shape having a maximum at approximately the recoil energy $\epsilon_R = \hbar^2 Q^2/2m$, the form expected for scattering from nearly free nuclei. To display this character we have plotted in Fig. 13, as a solid line, the position of the maximum of $S(\vec{Q}, \epsilon)$ and the position of one half the peak height on each side of the maximum, for Q along the [111] direction. This shows that for $Q > 2.5$ Å^{-1} the maximum lies close to the recoil energy $\epsilon_R = \hbar^2 Q^2/2m$. The os-

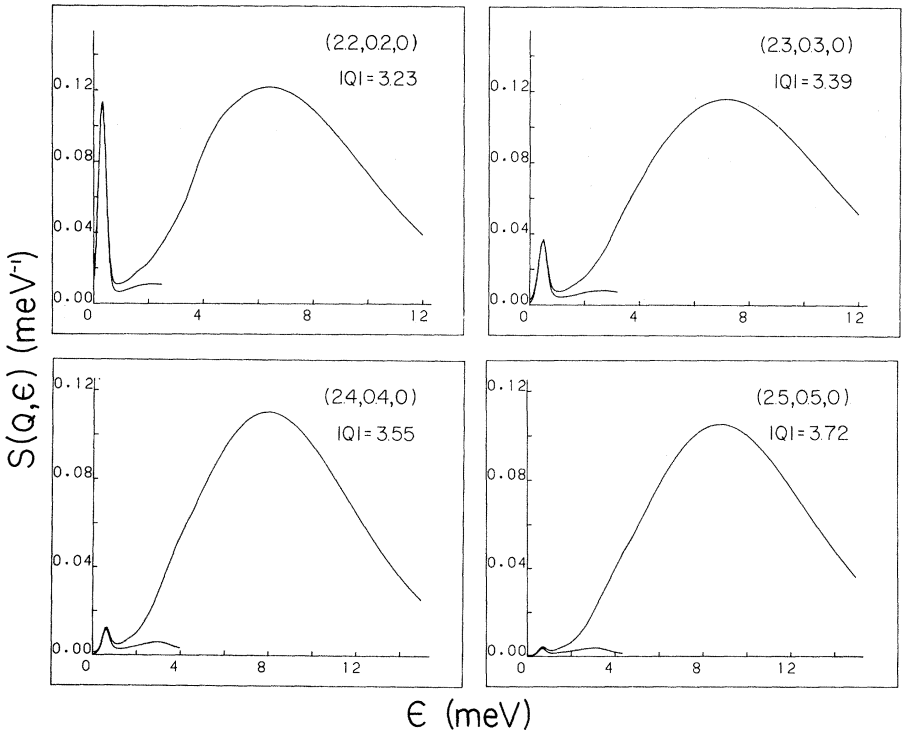

FIG. 12. As Fig. 11 for transverse phonons along $\vec{Q} = (2\pi/a)(2.\zeta, \zeta, 0)$, $\zeta = 0.2$–0.5.

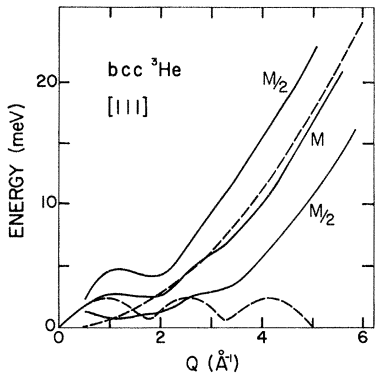

FIG. 13. The three solid lines show the position of the maximum (M) of $S(\vec{Q},\epsilon)$ and the position at which $S(\vec{Q},\epsilon)$ drops to one half its maximum value on each side of the maximum ($\frac{1}{2}M$), as a function of $\vec{Q}$. The upper dashed line shows the recoil energy $E_R=\hbar^2Q^2/2m$ while the lower shows the one-phonon dispersion curve.

cillating dashed line shows the dispersion curve expected for scattering from single phonons only and coincides with the maximum of $S(\vec{Q},\epsilon)$ only for $Q<0.8$ Å^{-1}. Similar results are obtained for the [100] and [110] directions.

For solid ^{4}He, Horner[44] obtained similar results at high Q using a self-consistent phonon theory as did Sears[35] using a continued-fraction approach usually applied to liquids. It is interesting that a multiphonon scattering picture looks identical to a nearly-free-particle scattering model.

In Fig. 14 we plot $S_c(\vec{Q})$ for the $\vec{Q}$ along the [110] and [111] directions. The $S(\vec{Q})$ along [110] has the familiar divergence expected in crystals at the Bragg point (110). However, along [111] the first Bragg point does not occur until (222) where $|Q|\approx 5$ Å^{-1}. At these large Q values $S(\vec{Q},\epsilon)$ is entirely dominated by multiphonon or single-free-particlelike scattering and $S(Q)$ does not show a divergence at the Bragg point (222) expected in crystals.

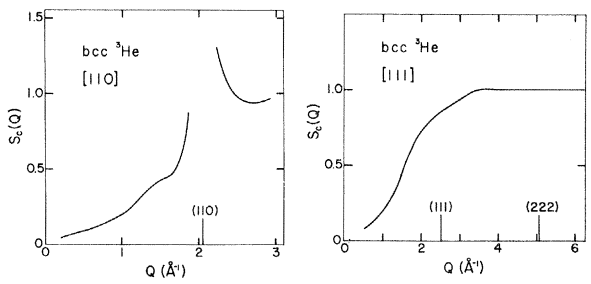

FIG. 14. The coherent static structure factor along the [110] and [111] directions predicted for bcc ^{3}He at $V=24$ cm^3/mole.

V. DISCUSSION

A. Interference and comparison with solid ^{4}He

The $S_c(\vec{Q},\epsilon)$ presented in Sec. IV contains substantial contributions from interference between the one- and two-phonon processes. These contributions can be best illustrated in combination with a comparison of the $S(\vec{Q},\epsilon)$ for solid ^{3}He and measurements[26] of neutron scattering from solid ^{4}He. In Fig. 15 we compare the pure one-phonon scattering component $S_1(\vec{Q},\epsilon)$ with the full one-phonon term

$$S_p(\vec{Q},\epsilon)=S_1(\vec{Q},\epsilon)+S_{12}(\vec{Q},\epsilon)\ ,$$

which includes the one- and two-phonon interference contribution for the longitudinal phonon at $\vec{Q}=(2\pi/a)(0.7,0,0)$. We see that including the interference term makes $S_p(\vec{Q},\epsilon)$ peak at a much higher frequency leading to an apparently much higher one-phonon frequency. This effect can be seen in the data of Osgood *et al.*,[26] shown in Fig. 16. They determined the apparent one-phonon frequencies from the peak position in the scattering intensity. The peak positions for longitudinal phonons along the [100] direction lie well above the values predicted by the SCH+C theory and well above that expected for one-phonon frequencies from a comparison with other symmetry directions. We believe the apparently large values observed for the one-phonon frequencies along the [100] direction is due to an interference effect. A comparison of Fig. 16 and Fig. 2 also shows the significant difference in $S_p(\vec{Q},\epsilon)$ computed using the SCH frequencies $\omega_{q\lambda}$ as intermediate propagator frequencies (Fig. 2) and the frequencies $\hat{\omega}_{q\lambda}$

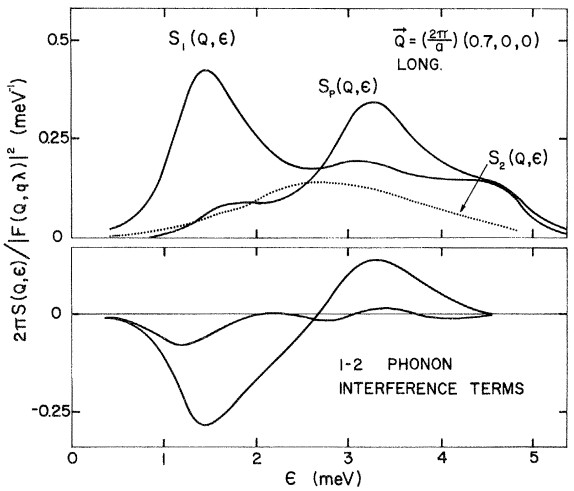

FIG. 15. The components of the coherent dynamic form factor (as in Fig. 2) calculated using the $\hat{\omega}_{q\lambda}$ frequencies as intermediate propagator frequencies.

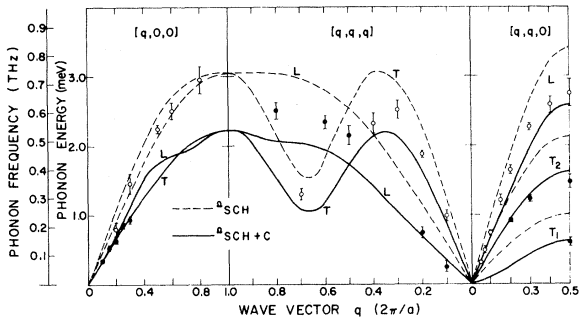

FIG. 16. The apparent one-phonon frequencies observed by Osgood *et al.* and the predicted one-phonon frequencies in the SCH and SCH+C approximations by Glyde and Khanna for bcc ^{4}He.

given by the mean position of $S_1(\vec{Q}, \omega)$ for each $q\lambda$ as the intermediate propagator frequencies (Fig. 16).

The effect of interference is further displayed in Figs. 17 and 18. The upper part of Fig. 17 shows the coherent $S_c(\vec{Q}, \omega)$ calculated for the longitudinal phonons at $\vec{Q} = (2\pi/a)(0.5, 0, 0)$ and $\vec{Q} = (2\pi/a)$

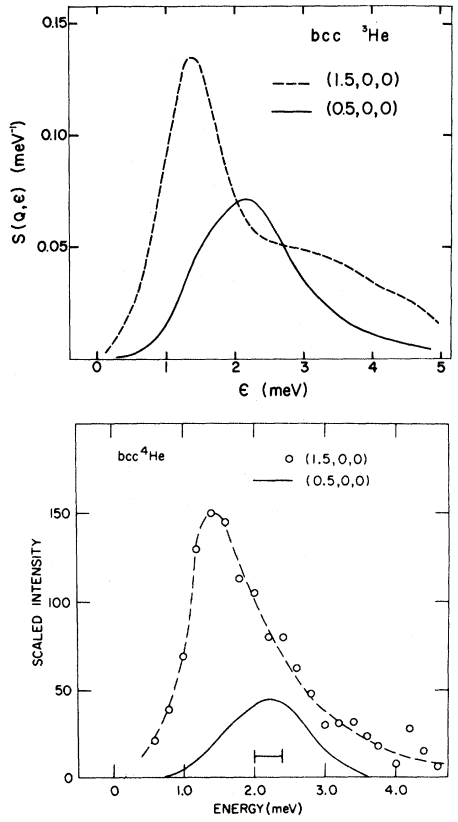

FIG. 17. The coherent $S_c(\vec{Q}, \epsilon)$ of longitudinal phonons predicted for solid ^{3}He (upper figure) compared with the scattering intensity observed from solid ^{4}He by Osgood *et al.*

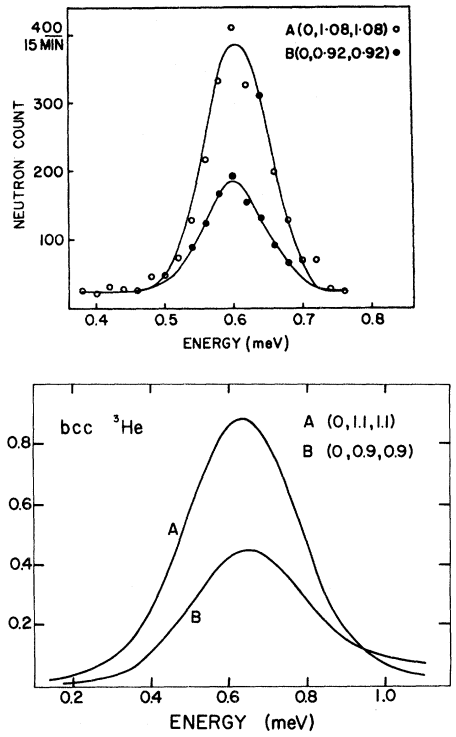

FIG. 18. The coherent $S_c(\vec{Q}, \epsilon)$ of longitudinal phonons predicted by bcc ^{3}He (lower figure) and the scattering intensity observed from bcc ^{4}He by Minkiewicz *et al.*

$\times (1.5, 0, 0)$ in bcc ^{3}He. Without interference these two $S_c(\vec{Q}, \omega)$ would peak at the same frequency and would be of approximately the same magnitude [see plot of $Q^2 d^2(Q)$ in Fig. 4]. The lower part of Fig. 17 shows the scattering intensity observed by Osgood *et al.*[26] at the same two wave vectors in bcc ^{4}He. The observed intensity clearly shows the interference contributions, as first pointed out by Horner.[29] The phonon linewidths are marginally broader in solid ^{3}He than in solid ^{4}He. Figure 18 shows a further intensity contribution from interference as calculated in bcc ^{3}He and observed by Minkiewicz *et al.*[26] in bcc ^{4}He. Without interference we expect the one-phonon intensity shown in Fig. 18 to be greater at point B than at point A.

B. Comparison with liquid ^{3}He

The magnitude of $S(\vec{Q}, \epsilon)$ predicted here for solid ^{3}He at $V = 24$ cm^3/mole (Figs. 7–12) is between 2 to 4 times smaller than that observed in liquid ^{3}He at saturated vapor pressure (SVP).[1] If the present calculations are correct this means neutron scattering from solid ^{3}He will be even more difficult to observe than from liquid ^{3}He at SVP. The smaller size of $S(\vec{Q}, \epsilon)$ in the solid can be understood on the basis

of the f-sum rule. The longitudinal phonon energies predicted here are two to three times greater than the zero sound mode energy at SVP.[1,2] The f-sum rule will therefore require the coherent part of $S(\vec{Q}, \omega)$ to be two to three times smaller at a given scattering vector $\vec{Q}$. Only the coherent part of the scattering satisfies the f-sum rule in the liquid.

A calculation[6] of $S(\vec{Q}, \epsilon)$ in the liquid using the Landau parameters to describe the effective ^{3}He quasiparticle-quasihole interaction suggests the zero sound mode energy in liquid ^{3}He under 30-atm pressure is comparable to the longitudinal phonon energy in solid ^{3}He shown in Fig. 3. If these calculations are correct the collective excitation energies in the liquid and solid are roughly the same near the melting line. The $S(\vec{Q}, \epsilon)$ for liquid ^{3}He near the solidification curve is also predicted to fall to the magnitude predicted here for solid ^{3}He near melting. Thus, although the models used to describe the solid and the liquid are quite different, $S(\vec{Q}, \epsilon)$ is predicted to be very similar in each near melting with the phonon groups being predicted to be somewhat sharper than the zero sound mode peak.

ACKNOWLEDGMENTS

It is a pleasure to acknowledge valuable discussions with R. A. Cowley, S. W. Lovesey, C. Pelizzari, K. Sköld and W. G. Stirling.

[1]W. G. Sterling, R. Scherm, V. Volino, and R. A. Cowley, in *Proceedings of the Fourteenth International Conference on Low Temperature Physics, Otaniemi, Finland,* edited by M. Krusius and M. Vuorio (North-Holland, Amsterdam, 1976); R. Scherm, W. G. Stirling, A. D. B. Woods, R. A. Cowley, and G. J. Coombs, J. Phys. C 1, L341 (1974); W. G. Stirling, R. Scherm, P. A. Hilton, and R. A. Cowley, J. Phys. C 9, 1643 (1976); P. A. Hilton, R. A. Cowley, W. G. Stirling, and R. Scherm, Z. Phys. B30, 107 (1978); W. G. Stirling, J. Phys. (Paris) 39, C6-1334 (1978); P. A. Hilton, R. A. Cowley, R. Scherm, and W. G. Stirling, J. Phys. C 13, L295 (1980).

[2]K. Sköld, C. A. Pelizzari, R. Kleb, and G. E. Ostrowski, Phys. Rev. Lett. 37, 842 (1976); K. Sköld and C. A. Pelizzari, in *Quantum Fluids and Solids,* edited by S. B. Trickey, E. D. Adams, and J. W. Duffy (Plenum, New York, 1977), p. 195; J. Phys. C 11, L589 (1978); Philos. Trans. R. Soc. London Ser. B, 290, 605 (1980).

[3]L. D. Landau, Zh. Eksp. Teor. Phys. 30, 1058 (1956) [Sov. Phys. JETP 3, 920 (1956)].

[4]D. Pines, in *Quantum Fluids,* edited by D. Brewer (North-Holland, Amsterdam, 1966), p. 257.

[5]C. H. Aldrich, III and D. Pines, J. Low Temp. Phys. 32, 689 (1978), and earlier references therein.

[6]H. R. Glyde and F. C. Khanna, Can. J. Phys. 58, 343 (1980), and earlier references therein.

[7]O. T. Valls, G. F. Mazenko, and H. Gould, Phys. Rev. B 18, 263 (1978); and (unpublished).

[8]S. Takeno and F. Yoshida, Prog. Theor. Phys. 60, 1585 (1978); F. Yoshida and S. Takeno, Prog. Theor. Phys. 62, 37 (1979).

[9]S. W. Lovesey, J. Phys. C 8, 1649 (1975); S. W. Lovesey and J. R. D. Copley, *International Symposium on Neutron Inelastic Scattering, Vienna, 1977* (IAEA, Vienna, 1977).

[10]M. T. Beal-Monod, J. Low Temp. Phys. 37, 123 (1979); J. Magn. Magn. Mater. 14, 283 (1979).

[11]W. P. Halperin, C. N. Archie, F. B. Rasmussen, R. A. Buhrmann, and R. C. Richardson, Phys. Rev. Lett. 32, 927 (1974); 34, 718 (1975).

[12]For reviews, see A. Landesman, J. Phys. (Paris) 39, C6-1305 (1978); R. A. Guyer, J. Low Temp. Phys. 30, 1 (1978).

[13]D. D. Osheroff, M. C. Cross, and D. S. Fischer, Phys. Rev. Lett. 44, 792 (1980); E. D. Adams, E. A. Schuberth, G. E. Haas, and D. M. Bakalyer, Phys. Rev. Lett. 44, 789 (1980).

[14]T. C. Prewitt and J. M. Goodkind, Phys. Rev. Lett. 44, 1699 (1980); H. Godfrin, G. Frossati, A. Greenberg, B. Hebral, and D. Thoulouse, Phys. Rev. Lett. 44, 1695 (1980).

[15]M. Roger, J. M. Delrieu, and J. H. Hetherington, Phys. Rev. Lett. 45, 137 (1980).

[16]W. Marshall and S. W. Lovesey, *Theory of Thermal Neutron Scattering,* (Oxford University Press, London, 1971), Chap. 7.

[17]P. F. Choquard, *The Anharmonic Crystal* (Benjamin, New York, 1967); T. R. Koehler, Phys. Rev. Lett. 17, 89 (1966); H. Horner, Z. Phys. 205, 72 (1967); N. Bocarra and G. Sarma, Physics (N.Y.) 1, 219 (1965).

[18]D. E. Beck, Mol. Phys. 14, 311 (1968).

[19]H. Horner, in *Dynamical Properties of Solids,* edited by G. K. Horton and A. A. Maradudin (North-Holland, Amsterdam, 1974), Vol. 1; T. R. Koehler, in *Dynamical Properties of Solids,* edited by G. K. Horton and A. A. Maradudin (North-Holland, Amsterdam, 1975), Vol. 2; H. R. Glyde, in *Rare Gas Solids,* edited by M. L. Klein and J. A. Venables (Academic, New York, 1976), Vol. 1; C. M. Varma and N. R. Werthamer, in *The Physics of Liquid and Solid Helium,* edited by K. H. Benneman and J. B. Ketterson (Wiley, New York, 1976), Vol. 1.

[20]H. R. Glyde and F. C. Khanna, Can. J. Phys. 50, 1143, 1152 (1972).

[21]V. J. Minkiewicz, T. A. Kitchens, F. P. Lipschultz, and G. Shirane, Phys. Rev. 174, 267 (1968); F. P. Lipschultz, V. J. Minkiewicz, T. A. Kitchens, G. Shirane, and R. Nathans, Phys. Rev. Lett. 19, 1307 (1967).

[22]R. A. Reese, S. K. Sinha, T. O. Brun, and C. R. Telford, Phys. Rev. A 3, 1688 (1971); T. O. Brun, S. K. Sinha, C. A. Swenson, and C. R. Tilford, in *Neutron and Inelastic Scattering* VI (IAEA, Vienna, 1968).

[23]J. G. Traylor, C. Stassis, R. A. Reese, and S. K. Sinha, in *Neutron Inelastic Scattering* (IAEA, Vienna, 1972).

[24]J. Eckert, W. Thomlinson, and G. Shirane, Phys. Rev. B 16, 1057 (1977); W. Thomlinson, J. Eckert, and G. Shirane, Phys. Rev. B 18, 1120 (1978).

[25]C. Stassis, G. Kline, W. A. Kamitakahara, and S. K. Sinha,

Phys. Rev. B 17, 1130 (1978).
[26]E. B. Osgood, V. J. Minkiewicz, T. A. Kitchens, and G. Shirane, Phys. Rev. A 5, 1537 (1972); T. A. Kitchens, G. Shirane, V. J. Minkiewicz, and E. B. Osgood, Phys. Rev. Lett. 29, 552 (1972); V. J. Minkiewicz, T. A. Kitchens, G. Shirane, and E. B. Osgood, Phys. Rev. A 8, 1513 (1973).
[27]V. Ambegaokar, J. Conway, and G. Baym, in *Lattice Dynamics,* edited by R. F. Wallis (Pergamon, New York, 1965), p. 261.
[28]R. A. Cowley, E. C. Svensson, and W. J. L. Buyers, Phys. Rev. Lett. 23, 325 (1969); R. A. Cowley and W. J. L. Buyers, J. Phys. C 2, 2262 (1969).
[29]H. Horner, Phys. Rev. Lett. 29, 556 (1972).
[30]N. R. Werthamer, Phys. Rev. Lett. 28, 1102 (1972).
[31]V. F. Sears and F. C. Khanna, Phys. Rev. Lett. 29, 549 (1972).
[32]H. R. Glyde, Can. J. Phys. 52, 2281 (1974).
[33]J. Meyer, G. Dolling, R. Scherm, and H. R. Glyde, J. Phys. F 6, 943 (1976).
[34]See Ref. 16, Sec. 3.5.
[35]V. F. Sears, Solid State Commun. 11, 1307 (1972).
[36]V. F. Sears, J. Phys. C 9, 409 (1976).
[37]V. F. Turchin, *Slow neutrons* (Israel Program for Scientific Translations, Jerusalem, Israel, 1965), p. 108.
[38]T. A. Kitchens, T. Oversluizen, L. Passell, and R. I. Schermer, Phys. Rev. Lett. 32, 791 (1974).
[39]L. Van Hove, Phys. Rev. 95, 249 (1954).
[40]Reference 16, p. 232 and L. Van Hove, Phys. Rev. 95, 1374 (1954).
[41]A. K. McMahan, J. Low Temp. Phys. 8, 115, 159 (1972).
[42]L. H. Nosanow and C. M. Varma, Phys. Rev. Lett. 20, 912 (1968); Phys. Rev. 187, 660 (1969).
[43]H. Horner, J. Low Temp. Phys. 8, 511 (1972).
[44]H. Horner, in *Proceedings of the Thirteenth International Conference on Low Temperature Physics,* edited by K. D. Timmerhaus, W. J. O'Sullivan, and E. F. Hammel (Plenum, New York, 1974).